

## High-Fidelity Hydrophilic Probe for Two-Photon Fluorescence Lysosomal Imaging

Xuhua Wang,<sup>†</sup> Dao M. Nguyen,<sup>†</sup> Ciceron O. Yanez,<sup>†</sup> Luis Rodriguez,<sup>†</sup> Hyo-Yang Ahn,<sup>†</sup> Mykhailo V. Bondar,<sup>§</sup> and Kevin D. Belfield<sup>\*,†,‡</sup>

Department of Chemistry and CREOL, The College of Optics and Photonics, University of Central Florida, Orlando, Florida 32816, and Institute of Physics, Prospect Nauki, 46, Kiev-28, 03094 Ukraine

Received June 29, 2010; E-mail: belfield@mail.ucf.edu

Ⓜ This paper contains enhanced objects available on the Internet at <http://pubs.acs.org/jacs>.

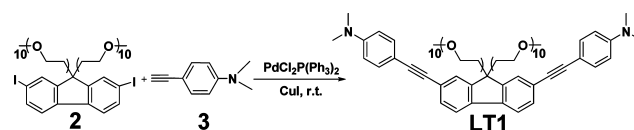
**Abstract:** The synthesis and characterization of a novel two-photon-absorbing fluorene derivative, LT1, selective for the lysosomes of HCT 116 cancer cells, is reported. Linear and nonlinear photophysical and photochemical properties of the probe were investigated to evaluate the potential of the probe for two-photon fluorescence microscopy (2PFM) lysosomal imaging. The cytotoxicity of the probe was investigated to evaluate the potential of using this probe for live two-photon fluorescence biological imaging applications. Colocalization studies of the probe with commercial LysoTracker Red in HCT 116 cells demonstrated the specific localization of the probe in the lysosomes with an extremely high colocalization coefficient (0.96). A figure of merit was introduced to allow comparison between probes. LT1 has a number of properties that far exceed those of commercial lysotracker probes, including higher two-photon absorption cross sections, good fluorescence quantum yield, and, importantly, high photostability, all resulting in a superior figure of merit. 2PFM was used to demonstrate lysosomal tracking with LT1.

Lysosomes are membrane-bound organelles of ~500 nm diameter that are terminal degradative compartments of mammalian cells.<sup>1</sup> Lysosomes are involved in numerous physiological processes, such as bone and tissue remodeling, plasma membrane repair, and cholesterol homeostasis, along with cell death and cell signaling.<sup>2</sup> In addition, tumor invasion and metastasis are largely associated with altered lysosomal trafficking, as are increased lysosomal enzyme expression and activity.<sup>3</sup> Effective techniques to fluorescently label lysosomes of cancer cells and solid tumor models are therefore of significant interest to study lysosomal trafficking and its role in invasion.<sup>4</sup>

In order to understand the biological activities of lysosomes, a limited number of fluorescent probes derived from Neutral Red (toluylene red) and Acridine Orange (*N,N,N',N'*-tetramethylacridine-3,6-diamine) have been developed.<sup>5</sup> However, most of the commercial probes require a rather short excitation wavelength, seriously limiting their use in tissue imaging due to low penetration depth, the need for biomolecular conjugation, pH sensitivity, poor water solubility, and poor photostability.<sup>6</sup> These limitations motivated us to search for two-photon-absorbing dyes for two-photon fluorescence microscopy (2PFM) imaging, since the longer wavelength (700–1000 nm) light and quadratic dependence on laser intensity of two-photon absorption (2PA) both provide advantages such as

highly localized excitation and prolonged observation time.<sup>7</sup> A biocompatible, photostable, and water-soluble lysosomal marker with high 2PA cross section will provide a strong tool to study lysosomal trafficking and its role in invasion with high-resolution spatial images.

### Scheme 1. Synthesis of Fluorene Derivative LT1



Herein, we describe a symmetric hydrophilic fluorene derivative, 4,4'-[9,9-di(2,5,8,11,14,17,20,23,26,29-decaoxahentriacontan-31-yl)-9*H*-fluorene-2,7-diyl]bis(ethyne-2,1-diyl)bis(*N,N*-dimethylaniline) (LT1), and demonstrate its use as an efficient 2PA fluorophore to perform noninvasive labeling of lysosomes *in vitro*. The new fluorene derivative LT1 was specifically designed to contain a pair of 10-unit polyethylene glycol (PEG) groups in the 9-position of the fluorene ring, which made the probe highly water-soluble and imparted very low cytotoxicity. The hydrophilic fluorene derivative LT1 was synthesized from the 2,7-diiodofluorene **2** and 4-ethynyl-*N,N*-dimethylaniline **3** through a Sonogashira cross-coupling reaction using a PdCl<sub>2</sub>P(Ph<sub>3</sub>)<sub>2</sub>/CuI catalytic system in 72% yield (Scheme 1).<sup>8</sup>

The linear and nonlinear photophysical properties of the probe are reported to investigate specific fluorescence characteristics that are important for nonlinear optical applications. The absorption and emission spectra of LT1 were sensitive to solvent polarity, and the emission spectra exhibited large bathochromic shifts in the order of toluene < THF < EtOH < H<sub>2</sub>O (Figure S1 and Table S1, Supporting Information). The emission spectra showed much greater solvatochromic shifts than absorption spectra (79 nm vs 7 nm), suggestive of the potential of LT1 as a polarity-sensitive probe.

In addition, the excitation anisotropy spectra and anisotropy values, *r*, for LT1 in polytetrahydrofuran (pTHF) are shown in Figure 1, along with the linear absorption spectra for LT1 in phosphate-buffered saline. Probe LT1 displayed a constant value of *r* ≈ 0.37 for excitation in the spectral range  $\lambda \approx 374$ –455 nm, corresponding to the first electronic transition S<sub>0</sub> → S<sub>1</sub>. A higher electronic transition, S<sub>0</sub> → S<sub>2</sub>, was observed in the wavelength range  $\lambda \approx 289$ –326 nm (*r* ≈ 0.24). Because the pH of lysosomes is ca. 4.8, pH stability in acidic environments is essential for lysosomal probes. The pH stability of LT1 was investigated by measuring the absorbance and emission of LT1 in a series of buffers with different pH values from 4.16 to 10.0. The results, illustrated in Figure S2 (Supporting Information), indicated that LT1 was very stable over this entire pH range.

<sup>†</sup> Department of Chemistry, University of Central Florida.

<sup>‡</sup> College of Optics and Photonics, University of Central Florida.

<sup>§</sup> Institute of Physics, Prospect Nauki.

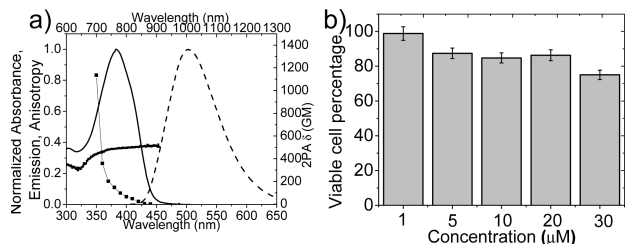


**Figure 1.** (a) Normalized absorption (solid line) (in PBS), emission (dashed line) (in PBS), and anisotropy (dotted line) spectra (in pTHF) and two-photon absorption cross section (squares) (in toluene) of LT1. (b) Viability of HCT 116 cells with LT1.

By employing a standard two-photon-induced fluorescence method with a femtosecond laser system, probe LT1 afforded a maximum 2PA cross section of  $\sim 1100$  GM ( $1 \text{ GM} = 10^{-50} \text{ cm}^4 \cdot \text{s} \cdot \text{photon}^{-1}$ ) at 700 nm (Figure 1a, squares), which is much higher than for commercial probes or those reported by others ( $<10$ – $200$  GM for 2PFM bioimaging).<sup>9</sup> In addition, the photostability and 2PA cross sections of LT1 were compared with those of the commercially available lysosomal markers LysoTracker Red (LT Red) and LysoTracker Green (LT Green) via photodecomposition experiments and 2PA cross section measurements. Herein, we define a figure of merit ( $F_M$ ) by which probes for 2PFM can be compared, calculated as the product of their fluorescence quantum yield ( $\Phi$ ) and 2PA cross section ( $\delta$ ) normalized by their photodecomposition quantum yield ( $\eta$ ), i.e.,  $F_M = \Phi\delta/\eta$ . The  $F_M$  of LT1 was 2 orders of magnitude higher than those of LT Green and LT Red (Table 1), providing strong support for the fidelity of LT1 relative to commercial lysotracker probes for 2PFM biological imaging.

**Table 1.** Photophysical Data for LT1, LysoTracker Green, and LysoTracker Red<sup>a</sup>

probe	$\lambda_{\text{max}}^{(1)}/\lambda_{\text{max}}^{(2)}$ <sup>b</sup>	$\epsilon^c$	$\Phi^d$	$\delta^e$	$\eta \times 10^6$ <sup>f</sup>	$\Phi\delta^g$	$F_M \times 10^{-6}$ <sup>h</sup>
LT1	387/501	7.7	0.38	1135	0.94	431.3	458.8
LT Green	502/510	6.3	1.0	17	3.70	17	4.6
LT Red	575/591	4.9	0.07	33	5.31	2.3	0.4

<sup>a</sup> Except for 2PA cross section measurements, all other measurements were performed in PBS buffer. <sup>b</sup>  $\lambda_{\text{max}}$  values of the one-photon absorption and emission spectra in nm. <sup>c</sup> Molar absorbance in  $1 \times 10^4 \text{ M}^{-1} \cdot \text{cm}^{-1}$ . <sup>d</sup> Fluorescence quantum yield,  $\pm 15\%$ . <sup>e</sup> 2PA cross section (LT1 in toluene at 700 nm, LT Green in DMSO at 700 nm, and LT Red in DMSO at 740 nm) in  $10^{-50} \text{ cm}^4 \cdot \text{s} \cdot \text{photon}^{-1}$  (GM),  $\pm 15\%$ . <sup>f</sup> Photobleaching decomposition quantum yield. <sup>g</sup> Product of fluorescence quantum yield and 2PA cross section in GM. <sup>h</sup> Figure of merit in GM.

In order to demonstrate the potential utility of LT1 for 2PFM cellular imaging, its cytotoxicity or cell viability must be assessed. To address this, viability assays in an epithelial colorectal carcinoma cell line, HCT 116, were conducted via the MTS assay.<sup>10</sup> Figure 1b shows the viability data for HCT 116 cells after treatment with several concentrations of LT1 for 24 h. The data indicate that LT1 has low cytotoxicity ( $\sim 85\%$  viability) over a concentration range from 1 to 20  $\mu\text{M}$ , appropriate for cell imaging. This bodes well for the utility of this hydrophilic probe, particularly in live cell imaging applications for lysosomal tracking via 2PFM.

Subsequently, in order to assess whether LT1 can be efficiently taken up by cancer cells, the uptake of LT1 by HCT 116 cells was evaluated. The one-photon fluorescence microscopy (1PFM) and 2PFM images showed LT1 can be effectively taken up by HCT 116 cells, and the optimum concentration of LT1 for cellular uptake was determined by comparing the images of HCT 116 treated with

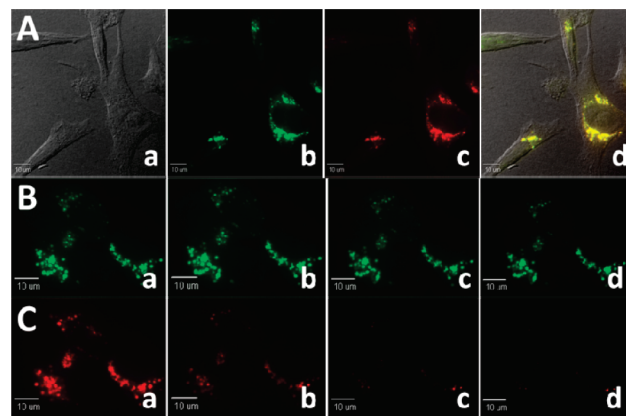


**Figure 2.** Colocalization images of HCT 116 cells incubated with LT1 (20  $\mu\text{M}$ , 2 h) and LysoTracker Red (LT Red, 75 nM, 2 h) and photostability comparison of LT1 and LT Red as lysosome markers in HCT 116 cells. Row A: (a) differential interference contrast (DIC) image, (b) one-photon confocal probe LT1 fluorescence image using a custom-made Fluor out filter cube (Ex 377/50, DM 409, Em 525/40), (c) one-photon confocal probe LT Red fluorescence image using a Texas Red filter cube (Ex 562/40, DM 593, Em 624/40), and (d) merged DIC image and two channels of fluorescence images. Rows B and C show one-photon confocal microscopy images of HCT 116 cells co-stained with (B) LT1 and (C) LT Red. The images were taken at (a) 0, (b) 6, (c) 12, and (d) 15 min under successive irradiation; the power on the focus plane was  $\sim 9$  mW. All images were acquired with a  $60\times$  oil immersion objective.

5, 10, 20, and 30  $\mu\text{M}$  LT1 for 2 h. The results demonstrate that HCT 116 treated with 20  $\mu\text{M}$  provides bright images with negligible toxicity.

In addition, to determine the location of the probes in the cells, a colocalization study of LT1 with several well-known one-photon fluorescence probes in HCT 116 cells was conducted. 1PFM images of HCT 116 cells co-stained with LT1 and LT Red, mitochondrion marker MitoTracker Red FM (MT), or Golgi apparatus marker Alexa Fluor 555 (AF) (Figure 2 and Figure S6, Supporting Information) individually demonstrated that the localization of LT1 in the cells was nearly identical to that of LT Red. The 1PFM images of HCT 116 cells were obtained with two different channels: Fluor out [excitation filter (Ex) 377/50, where 377 means the transmission maximum is 377 nm and 50 represents bandwidth of 50 nm, i.e.,  $377 \pm 25$  nm; dichroic mirror (DM) 409 (this is a long-pass filter/mirror, with a cutoff at 409 nm, thereby reflecting all light  $<409$  nm and transmitting light  $>409$  nm); emission filter (Em) 525/40, i.e., transmission maximum  $525 \pm 20$  nm] for LT1 and Texas Red [Ex 562/40; DM 593; Em 624/40] for commercial markers under the same conditions. The colocalization coefficient,  $A$ , was calculated by using Slidebook 5.0 software with Pearson's method to evaluate the colocalization of LT1 relative to the commercial probes. The data in Table S2 (Supporting Information) show that the colocalization coefficient of LT1 with LT Red was much higher than the others (0.96 vs 0.45, 0.46), indicating that LT1 possesses lysosomal specificity.

Moreover, the photostability of LT1 and LT Red in the HCT 116 cells was also compared (Figure 2 and Figure S9, Supporting Information) and was consistent with the photodecomposition experiments in PBS buffer. The fluorescence intensity of LT Red decreased by ca. 50% in the first 3 min under successive irradiation using a 100 W mercury lamp (the power on the focal plane was  $\sim 9$  mW), resulting in only 10% of the initial fluorescence intensity after 15 min irradiation. In contrast, the fluorescence intensity of LT1 decreased very slowly to ca. 70% of the initial fluorescence intensity after 15 min irradiation. In order to evaluate if LT1 can be used as a long-term lysosome tracking probe, a long-term

lysosome tracking assay was conducted. The results (Figure S10, Supporting Information) revealed that 9 h after incubation the images still showed the probe was lysosome-specific, with a Pearson's colocalization coefficient of 0.78. This result demonstrates the potential for LT1 as a stable lysosome marker for two-photon fluorescence microscopy. An endocytosis process is proposed (Figure S8, Supporting Information) as a possible pathway of LT1 cellular uptake, consistent with the literature.<sup>11</sup>

In a next step, to get an initial sense of the lysosomal specificity of LT1 in other cell lines, COS-7 (African green monkey kidney fibroblast-like) cells were employed using the same method described above for the HCT 116 cells. The colocalization images (Figure S7, Supporting Information) and colocalization coefficient data (Table S2, Supporting Information) indicated that LT1 can also specifically label lysosomes of other cells and significantly avoid staining other organelles such as the Golgi apparatus and mitochondria, suggesting broad, general utility for this new probe.

To demonstrate the advantage of using probe LT1 as a lysosomal marker for 2PFM imaging, two-photon fluorescence imaging of HCT 116 cells was conducted. The HCT 116 cell images (Figure 3) indicate that the 1PFM and 2PFM images are similar, with higher 3D resolution and contrast realized by 2PFM, to the point of visualizing individual lysosomes, a feature rarely observed with other lysosomal probes.

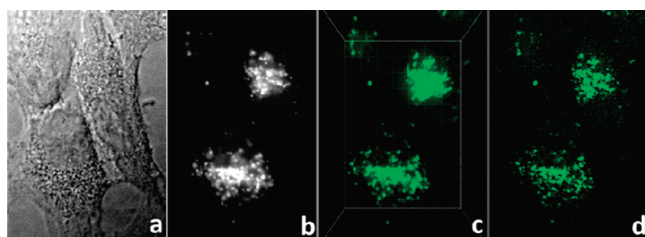


**Figure 3.** Images of HCT 116 cells incubated with fluorescence probe LT1 (20  $\mu$ M, 2 h), all taken with a 60 $\times$  oil immersion objective: (a) DIC, 500 ms; (b) one-photon fluorescence image, 150 ms (filter cube Ex 377/50, DM 409, Em 525/40); (c) 3D reconstruction from overlaid two-photon fluorescence images (Ex, 700 nm; Em, long-pass filter, 690 nm), 5  $\mu$ m grid; and (d) two-photon fluorescence image (Ex, 700 nm; Em, short-pass filter, 690 nm).

Ⓜ A movie showing a 3D rotation of the image in panel c is available in the HTML version.

In conclusion, we present a very effective hydrophilic fluorene derivative, LT1, as a lysosomal marker for two-photon fluorescence cell imaging. A figure of merit was introduced to allow comparison between probes. The new probe has a number of properties that

far exceed those of commercial lysotracker probes, including higher 2PA cross section, high lysosomal selectivity, good fluorescence quantum yield, and, importantly, high photostability, all resulting in a superior figure of merit. 2PFM was used to demonstrate lysosomal tracking with LT1, paving the way for future studies with LT1 to detect aberrant lysosomal trafficking. This may eventually lead to a new agent for studying lysosome-related diseases such as Tay-Sachs disease, mucopolysaccharidosis III B, and Niemann-Pick disease.<sup>12</sup>

**Acknowledgment.** This work was supported by the National Institutes of Health (1 R15 EB008858-01), the National Science Foundation (CHE-0832622 and CHE-0840431), the U.S. Civilian Research and Development Foundation (UKB2-2923-KV-07), and the Ministry of Education and Science of Ukraine (grant M/49-2008).

**Supporting Information Available:** Experimental details, <sup>1</sup>H and <sup>13</sup>C spectra, pH sensitivity measurements, photostability measurements, 2PA cross section determination, cytotoxicity assay, cell incubation conditions, colocalization studies, *in vitro* photostability, long-term lysosome tracking, and 2PFM lysosomal imaging (Figures S1–S10, Tables S1 and S2). This material is available free of charge via the Internet at <http://pubs.acs.org>.

## References

- (1) Luzio, J. P.; Pryor, P. R.; Bright, N. A. *Nat. Rev.* **2007**, *8*, 622–632.
- (2) Safig, P.; Klumperman, J. *Nat. Rev.* **2009**, *10*, 623–635.
- (3) Fehrenbacher, N.; Jäättelä, M. *Cancer Res.* **2005**, *65*, 2993–2995.
- (4) Glunde, K.; Foss, C. A.; Takagi, T.; Wildes, F.; Bhujwala, Z. *Bioconjugate Chem.* **2005**, *16*, 843–851.
- (5) Anderson, R. G. W.; Orci, L. *J. Cell Biol.* **1988**, *106*, 539–543.
- (6) (a) Lemieux, B.; Percival, M. D.; Falgueyret, J. *Anal. Biochem.* **2004**, *327*, 247–251. (b) Griffiths, G.; Hoflack, B.; Simons, K.; Mellman, I.; Kornfeld, S. *Cell* **1988**, *52*, 329–341.
- (7) Morales, A. R.; Yanez, C. O.; Schafer-Hales, K. J.; Marcus, A. I.; Belfield, K. D. *Bioconjugate Chem.* **2009**, *20*, 1992–2000.
- (8) Liang, Y.; Xie, Y.-X.; Li, J.-H. *J. Org. Chem.* **2006**, *71*, 379–381.
- (9) (a) Kim, M. K.; Lim, C. S.; Hong, J. T.; Han, J. H.; Jang, H. Y.; Kim, H. M.; Cho, B. R. *Angew. Chem., Int. Ed.* **2010**, *49*, 364–367. (b) Gao, Y.; Wu, J.; Li, Y.; Sun, P.; Zhou, H.; Yang, J.; Zhang, S.; Jin, B.; Tian, Y. *J. Am. Chem. Soc.* **2009**, *131*, 5208–5213. (c) Picot, A.; D'Aléo, A.; Baldeck, P. L.; Grichine, A.; Duperray, A.; Andraud, C.; Maury, O. *J. Am. Chem. Soc.* **2008**, *130*, 1532–1533.
- (10) Malich, G.; Markovic, B.; Winder, C. *Toxicology* **1997**, *124*, 179–192.
- (11) (a) Dunn, W. A., Jr. *J. Cell Biol.* **1990**, *110*, 1923–1933. (b) Helenius, A.; Mellman, I.; Wall, D.; Hubbard, A. *Trends Biochem. Sci.* **1983**, *8*, 245–250. (c) Lawrence, B. P.; Brown, W. J. *J. Cell Sci.* **1992**, *102*, 515–526.
- (12) (a) Ohmi, K.; Kudo, L. C.; Ryazantsev, S.; Zhao, H.; Karsten, S. L.; Neufeld, E. F. *Proc. Natl. Acad. Sci. U.S.A.* **2009**, *106*, 8332–8337. (b) Kirkegaard, T.; Roth, A. G.; Petersen, N. H. T.; Mahalka, A. K.; Oslén, O. D.; Moilanen, I.; Zylitz, A.; Knudsen, J.; Sandhoff, K.; Arenz, C.; Kinnunen, P. K. J.; Nylandsted, J.; Jäättelä, M. *Nature* **2010**, *463*, 549–554.

JA1057423